Magnetocrystalline anisotropy and coercivity of $Sm_2Fe_{15-x}Cu_xSi_2C$ (x = 0 and 1)

1998 J. Phys.: Condens. Matter 10 9359

(http://iopscience.iop.org/0953-8984/10/41/017)

J. Phys.: Condens. Matter **10** (1998) 9359–9367. Printed in the UK PII: S0953-8984(98)92538-3

Magnetocrystalline anisotropy and coercivity of $Sm_2Fe_{15-x}Cu_xSi_2C$ ($x = 0$ and 1)

Hong-wei Zhang†§, Shao-ying Zhang†, Bao-gen Shen†, Fang-wei Wang† and Ji-fan Hu‡

† State Key Laboratory of Magnetism, Institute of Physics and Centre for Condensed Matter Physics, Chinese Academy of Sciences, Beijing 100080, People's Republic of China
‡ Physics Department, Shandong University, Jinan 250100, People's Republic of China

Received 17 March 1998, in final form 1 July 1998

Abstract. Hard direction magnetization recoil curves were analysed taking into account the angular distribution of grain axes for textured $Sm_2Fe_{15-x}Cu_xSi_2C$ ($x = 0$ and 1) samples. Magnetocrystalline anisotropy constants K_1 and K_2 were determined in the temperature range between 1.5 K and 300 K using the textured samples. The anisotropy field was examined by the singular point detection technique results at room temperature. A maximum value of intrinsic coercivity $\mu_{0i}H_c$ around 1.02 T and 1.24 T at room temperature was obtained for $x = 0$ and 1 ribbons, respectively. The mechanism of coercivity was mainly controlled by the nucleation of reversed domains. The micro-structural parameter α_k and the averaged local effective demagnetization factor N_{eff} were derived from the temperature dependence of the coercivity.

1. Introduction

After the discovery of the gas-phase interstitial modification (GIM) process, it was found that interstitial Sm_2Fe_{17} nitrides and carbides have dramatically improved magnetic properties over those of the parent compounds, making them suitable candidates for permanent magnets [1, 2]. The problems of these carbides are their thermal instability by GIM and low carbon contents by direct arc-melting, making it difficult for those materials to reach a commercially applicable stage. In recent years, it was found that the substitution of Fe with an element such as Ga, Al, Si or Cr can stabilize the high carbon content R_2Fe_{17} carbides up to high temperature [3–7]. High coercivity has been obtained in $Sm_2(FeM)_{17}C_x$ (M = Cr, Ga, Al and Si) by melt-spinning or mechanical alloying techniques [7–13].

Our previously studies have shown that small Cu additions are very effective in enhancing the coercivity of Sm–Fe–Si–C ribbons. Up to now, the temperature dependence of the anisotropy constants K_1 and K_2 of $Sm_2(FeSi)_{17}C_y$ is not well known and single crystals for their precise determination are not available. In this paper, the temperature dependence of magneto-crystalline anisotropy constants K_1 and K_2 for $Sm_2Fe_{15-x}Cu_xSi_2C$ ($x = 0$ and 1) compounds were measured and analysed. The coercivity mechanism for $Sm_2Fe_{15-x}Cu_xSi_2C$ ribbons was studied.

§ E-mail address: zhjx@aphy02.iphy.ac.cn.

0953-8984/98/419359+09$19.50

2. Experimental details

The ingots of $Sm_2Fe_{15-x}Cu_xSi_2C$ ($x = 0$ and 1) were prepared by arc-melting the constituent materials Sm, Fe, Cu and Si (with a purity of at least 99.9%) and Fe–C alloy (5.2 wt% C and 94.4% Fe) under high purity argon gas. Due to a loss of Sm during the arc-melting, an excess of 20% Sm was added for compensation. The arc-melted ingots were homogenized in a vacuum quartz tube at 1323 K for 50 h, and then pulverized to powders of about 1 μm. The textured samples were prepared by mixing the powder with epoxy resin followed by aligning in a field of $\mu_0 H = 1.0$ T. The textured samples were cylinders of length 8 mm and diameter 3 mm; the demagnetizing field can then be easily calculated. The hard magnetic ribbons were made by using the melt-spinning technique with surface velocity of the Cu wheel around 30 m s^{-1}. The ribbons were annealed in vacuum at 873–1023 K for 15 min to crystallize and develop a fine microstructure.

X-ray diffraction (XRD) was used for identification of the single phase and for determining the crystallographic structure. The XRD measurements were carried out in a Rigaku Rint 1400 by using Cu Kα radiation. The theoretical density around 7.6×10^3 kg m^{-3} was obtained for both $x = 0$ and 1.

The initial magnetization curves were measured along and perpendicular to the aligning-field direction by an extracting sample magnetometer (ESM) with a magnetic field $\mu_0 H$ up to 6.5 T from 1.5 K to room temperature (RT). The magnetization recoil curve and demagnetization curve were measured by a SQUID with a maximum field $\mu_0 H_{max} = 7$ T from 1.5 K to RT. The magnetocrystalline anisotropy field H_A at RT was examined by the singular point detection (SPD) technique. Some magnetization hysteresis loops at RT were measured by a VSM with a maximum field $\mu_0 H_{max} = 2$ T. The saturation magnetization M_s is obtained by fitting the magnetization curves measured along the aligning-field direction according to the approach to the saturation law: $M(H) = M_s(1 - a/H - b/H^2)$.

3. Results and discussion

XRD measurements show that all samples have a single phase with the Th_2Zn_{17} structure except some ribbons with a small amount of α-Fe. Figure 1 shows the magnetization curves of the $x = 0$ sample measured at RT for increasing and decreasing magnetic fields with the magnetic field applied perpendicular to the alignment axis. Hard direction remanent magnetization M_r^H is a measure of the misaligned regions which have easy axes nearly parallel to the field rather than normal to it, and a perfectly textured sample would be expected to show $M_r^H = 0$. Because of non-zero remanence, the sample was partially textured. Assuming the distribution of the c-axis around the aligning direction is described by a Gaussian [14],

$$P(\xi) = P_0 \exp(-2\xi^2/w^2) \tag{1}$$

where ξ is the angle between the c-axis of the crystal and the direction of the alignment field axis, w is the degree of misalignment and P_0 is a normalization constant. It is a good approximation to substitute $P(\xi)$ with $P(\theta_H)$ of a plane parallel to the alignment [15], where θ_H is the angle between the c-axis of the crystal and the applied magnetic field. The value of M_r^H is used to obtain the w of $P(\theta_H)$, and $w \approx 20.0^\circ$ is achieved. The values of M_s, M_r^H and H_A at various temperatures of $Sm_2Fe_{15-x}Cu_xSi_2C$ ($x = 0$ and 1) compounds are given in table 1. The texture parameter M_r^H/M_s slightly increases with the decrease of temperature. This is mainly caused by experimental errors because the value of the anisotropy field at low temperature is much higher than the applied magnetic field.

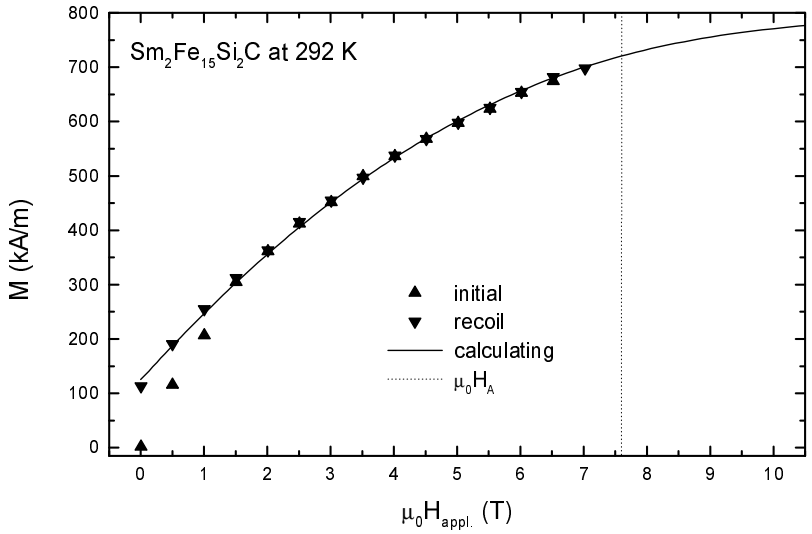

Figure 1. Experimental (initial and recoil) and calculated magnetization curves perpendicular to the alignment axis of $Sm_2Fe_{15}Si_2C$ at 293 K; dotted lines are related to the anisotropy field.

Table 1. The data of $M_s(T)$, $M_r^H(T)$ and $H_A(T)$ of $Sm_2Fe_{15-x}Cu_xSi_2C$ compounds, respectively.

		$T = 1.5$ K	$T = 50$ K	$T = 100$ K	$T = 150$ K	$T = 200$ K	$T = 250$ K	$T = 293$ K
	M_s (kA m^{-1})	933.3	915.0	895.0	873.5	850.6	828.6	819.3
$x = 0$	M_r^H (kA m^{-1})	—	163.5	154.1	140.8	133.8	122.4	112.7
	$\mu_0 H_A$ (T)[a]	16.1/17.8	14.9/16.4	13.6/15.3	12.1/13.7	9.9/11.8	8.4/10.6	7.6/8.5
	M_s (kA m^{-1})	869.4	851.2	833.9	815.0	798.3	782.2	769.9
$x = 1$	M_r^H (kA m^{-1})	—	159.3	144.4	135.2	122.1	113.5	99.1
	$\mu_0 H_A$ (T)[a]	16.1/17.8	14.6/16.5	13.2/15.5	11.5/13.7	10.3/11.7	8.4/10.4	7.5/8.5

[a] Taken from [13].

It is well known that the total free energy of the system is composed of the crystalline anisotropy energy and the magnetostatic energy giving:

$$F = K_1 \sin^2\theta + K_2 \sin^4\theta - \mu_0 M_s H \cos(\varphi - \theta) \tag{2}$$

where θ denotes the angle between the spontaneous magnetization M_s and the c-axis, and φ the angle between the applied magnetic field H and the c-axis.

The equilibrium condition for θ is given by $\delta F = 0$, and then the magnetic field H and the component of magnetization parallel to $\boldsymbol{H}$ are given by

$$H = (2K_1 \sin\theta\cos\theta + 4K_2 \sin^3\theta\cos\theta)/\mu_0 M_s \sin(\varphi - \theta) \tag{3}$$

$$M = M_s \cos(\varphi - \theta). \tag{4}$$

As $\varphi = \pi/2$, we can obtain the method commonly used to determine K_1 and K_2 provided by Sucksmith and Thompson. But this method only holds for a single crystal or perfectly textured powder samples. For non-ideal textured powder samples, this misalignment leads

to curvatures of the magnetization curve similar to those that would be produced by the effect of a larger value of K_2.

The non-zero remanence in the hard direction of magnetization for textured MnAlC and NdFeB samples has been discussed by Ram and Gaunt [16] and Durst and Kronmüller [15], respectively. In this paper, for the textured sample with Gauss distribution of individual c-axes, the total anisotropic energy F_K is used in equation (2) due to $F_K \sim \sin\theta$, and the magnetostatic energy is substituted by $\mu_0 M_s H \Sigma P \cos(\varphi^i - \theta)$. So equations (3) and (4) are changed as follows:

$$H = (2K_1 \sin\theta \cos\theta + 4K_2 \sin^3\theta \cos\theta)/[\mu_0 M_s \Sigma P \sin(\varphi^i - \theta)] \tag{5}$$

$$M = M_s \Sigma P \cos(\varphi^i - \theta). \tag{6}$$

Here the summation is taken over all grains and φ^i denotes the angle between the c-axis of grain i and the applied field $\boldsymbol{H}$. Equation (5) is an approximation working only for sufficiently well textured samples.

H_A can be given by

$$H_A = (2K_1 + 4K_2)/\mu_0 M_s. \tag{7}$$

The experimental recoil magnetization curve in the perpendicular direction can be perfectly fitted with equations (5) and (6) by using the angle distribution. As an example, it is shown in figure 1.

Figure 2 shows the temperature dependence of K_1 and K_2 determined from fits of the recoil curves in the temperature range from 1.5 K to RT. K_1 dramatically decreases with increasing temperature, while K_2 almost remains constant. The value of K_2 may be reliable in this study, just because good results of K_1 and K_2 dependence on temperature were obtained in a textured $Nd_2Fe_{14}B$ magnet by a similar method as given in the literature [15]. The temperature dependence of K_2 of $Sm_2Fe_{15-x}Cu_xSi_2C$ ($x = 0$ and 1) is quite different from that of $Sm_2Fe_{17}N_\delta$ ($\delta \approx 3$) compounds [17, 18], which maybe due to the different interstitial atom content and different valence electron charge between C and N. The values of H_A given by equation (7) are listed in table 1.

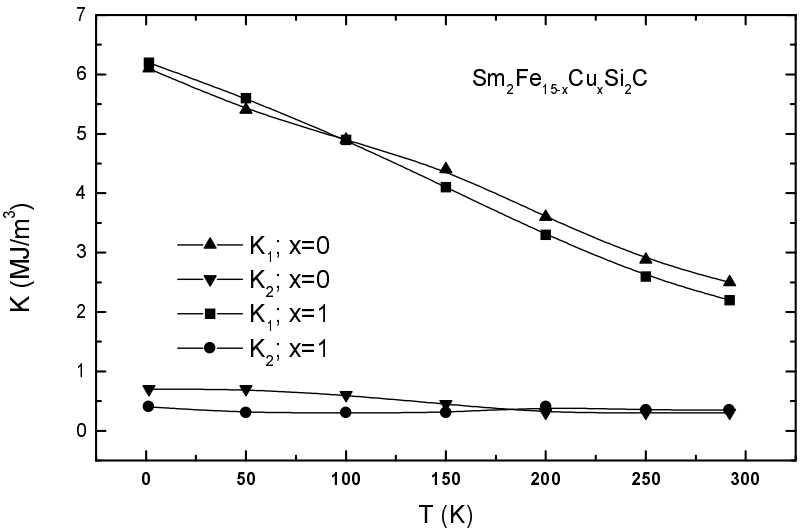

Figure 2. Temperature dependence of K_1 and K_2 for $Sm_2Fe_{15-x}Cu_xSi_2C$ ($x = 0$ and 1).

Figure 3 shows the SPD results of samples where the second derivative d^2M/dt^2 is plotted against the external field H at RT. The SPD signals associated with H_A are very strong, so that the experimental errors are minimized and the uncertainty in the values of $\mu_0 H_A$ is less than 0.2 T. The values of $\mu_0 H_A$ are 7.5 and 7.4 T for $x = 0$ and 1, respectively.

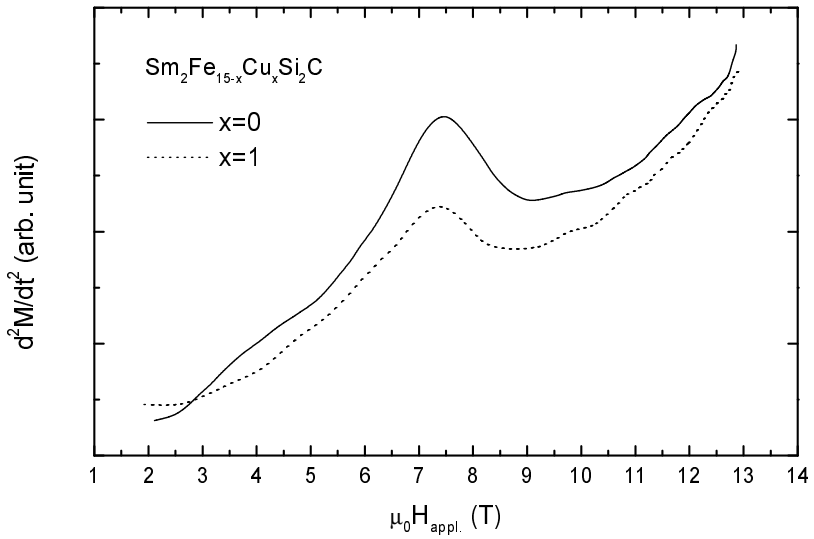

Figure 3. SPD signals: d^2M/dt^2 against external magnetic field $H_{appl.}$ at 293 K for $Sm_2Fe_{15-x}Cu_xSi_2C$ ($x = 0$ and 1).

The value of H_A obtained at RT by the calculation from K_1 and K_2 is good compared with the results of SPD, while the anisotropy field determined by the intersection point of the two magnetization curves measured along and perpendicular to the aligning-field direction [13] is higher than that of SPD and the calculated results. This may be due to the high curvatures of the perpendicular one caused by partial alignment.

Figure 4 exhibits the coercivity field ${}_iH_c$ dependence on the annealing temperature T_a of $Sm_2Fe_{15-x}Cu_xSi_2C$ ($x = 0$ and 1) ribbons. ${}_iH_c$ was determined by the VSM. The values of ${}_iH_c$ first increase slightly with increasing T_a, and achieve a maximum value of $\mu_{0i}H_c$ around 1.0 T and 1.2 T for $x = 0$ and 1 ribbons at 923 K, respectively, then decrease with further increasing T_a. This can be explained by the dependence of coercivity on T_a.

Figure 5 shows the applied magnetizing field $H_{appl.}$ dependence of ${}_iH_c$ at RT for ribbons ($x = 0$ and 1) obtained at $T_a = 923$ K, respectively. The coercivities first increase with the increase of $H_{appl.}$. After $\mu_0 H_{appl.} = 1.9$ T, both the values of ${}_iH_c$ almost remain constant. A value of $\mu_{0i}H_c$ around 1.02 and 1.24 T in the field of ($\mu_0 H_{appl.}$) 7 T is achieved for $x = 0$ and 1 ribbons, respectively. We can conclude that the mechanism of coercivity is mainly controlled by the nucleation of reversed domains which is common in the nucleation-type magnet described by Buschow [19].

The dependence of ${}_iH_c$ and remanence on temperature for ribbons obtained at $T_a =$ 923 K is shown in figure 6. Values of m_r ($=M_r/M_s$) range from 0.49 to 0.52 at various temperatures. Some values of m_r are higher than the theoretical limit of 0.5 as predicted by Stoner and Wohlfarth [20]. The remanence enhancement is attributed to the inter-grain exchange interaction which is predominant in nanocrystalline magnets [21, 22]. The crystalline size in the ribbons after annealing is about 30–60 nm examined by the Scherrer method.

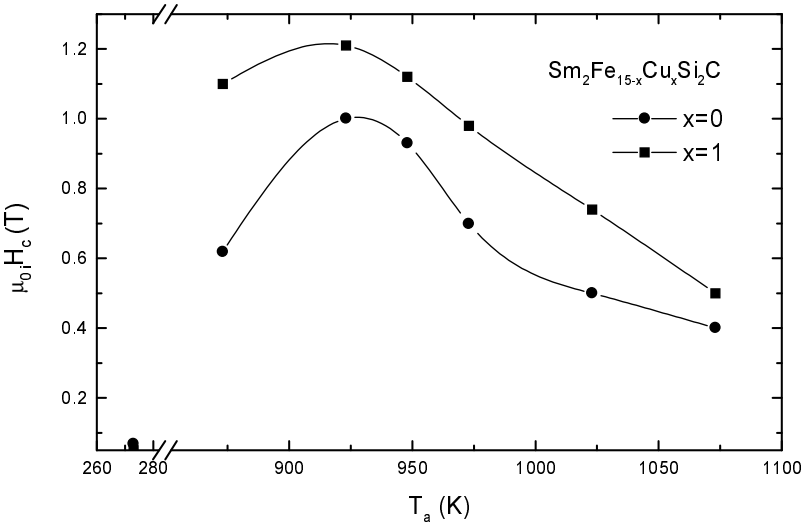

Figure 4. Intrinsic coercivity ${}_iH_c$ as a function of annealing temperature T_a for $Sm_2Fe_{15-x}Cu_xSi_2C$ ($x = 0$ and 1) ribbons obtained at wheel speed 30 m s^{-1}.

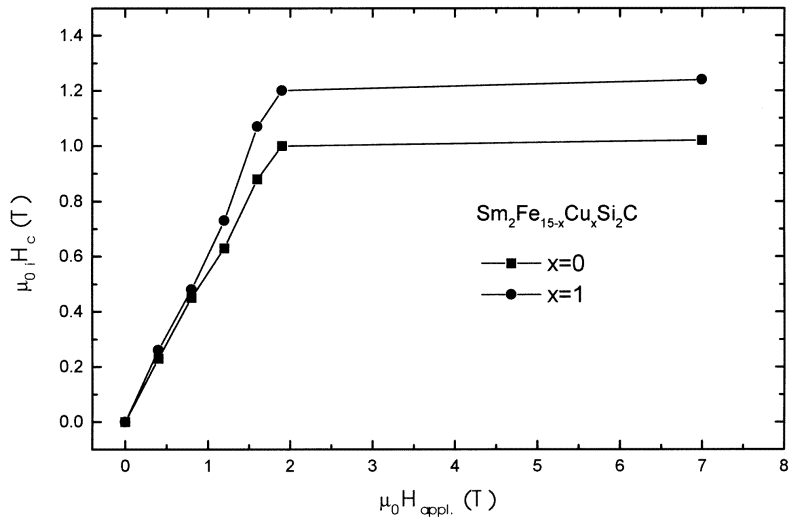

Figure 5. The dependence of intrinsic coercivity ${}_iH_c$ on external magnetic field $H_{appl.}$ for $Sm_2Fe_{15-x}Cu_xSi_2C$ ($x = 0$ and 1) ribbons obtained at 923 K.

Figure 7 shows the relationship of ${}_iH_c/M_s$ and H_A/M_s according to the nucleation-type magnet for $x = 0$ and 1 ribbons obtained at $T_a = 923$ K as follows

$$ {}_iH_c/M_s = \alpha H_A/M_s - N_{eff}. \tag{8}$$

Here α is the micro-structural parameter, N_{eff} is the averaged local effective demagnetization factor. The α can be written in the form $\alpha = \alpha_k\alpha_\varphi$, where α_k depends on the nature and size of the defect regions in which nucleation or pinning take place, and α_φ

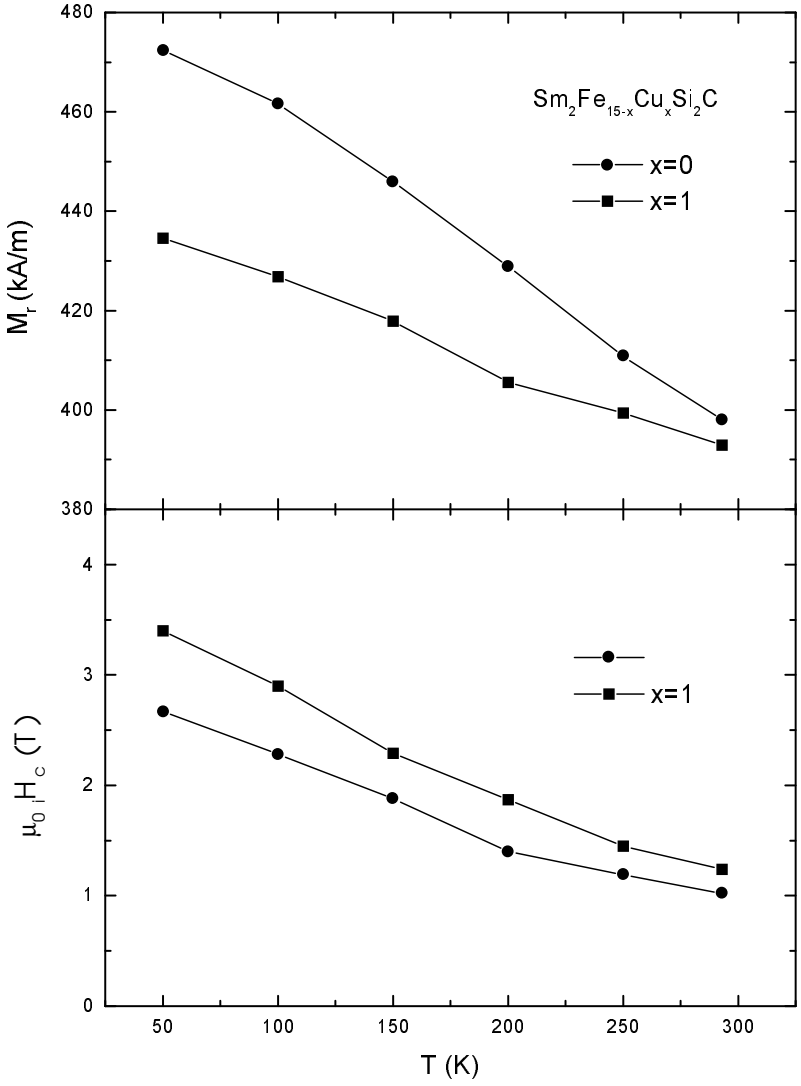

Figure 6. Temperature dependence of remanence M_r and intrinsic coercivity ${}_iH_c$ for $Sm_2Fe_{15-x}Cu_xSi_2C$ ($x = 0$ and 1) ribbons obtained at 923 K.

takes account of the misalignment of the grains in the magnet [23]. In isotropic ribbons, there is a rather good approximation α_φ for $\varphi = 45^\circ$, that is $\alpha_\varphi \approx 1/(\cos^{2/3}\varphi + \sin^{2/3}\varphi)^{3/2} = 0.5$ [20].

As demonstrated by figure 7, a linear relation is found over a larger temperature range. The value of α_k is 0.46 and 0.64 for $x = 0$ and 1 ribbons, respectively. The smaller value of α_k indicates that the inhomogeneous layer on the grain surface in $x = 0$ ribbons is thicker than that in $x = 1$ ribbons. N_{eff} is 0.77 and 1.30 for $x = 0$ and 1 samples, respectively. Such large local demagnetizing factors, helping to invert the magnetization and reduce ${}_iH_c$, can be expected near non-magnetic inclusions and sharp edges of the grains. In $x = 1$, the value of N_{eff} is nearly twice as large as that in $x = 0$ ribbon; a possible explanation

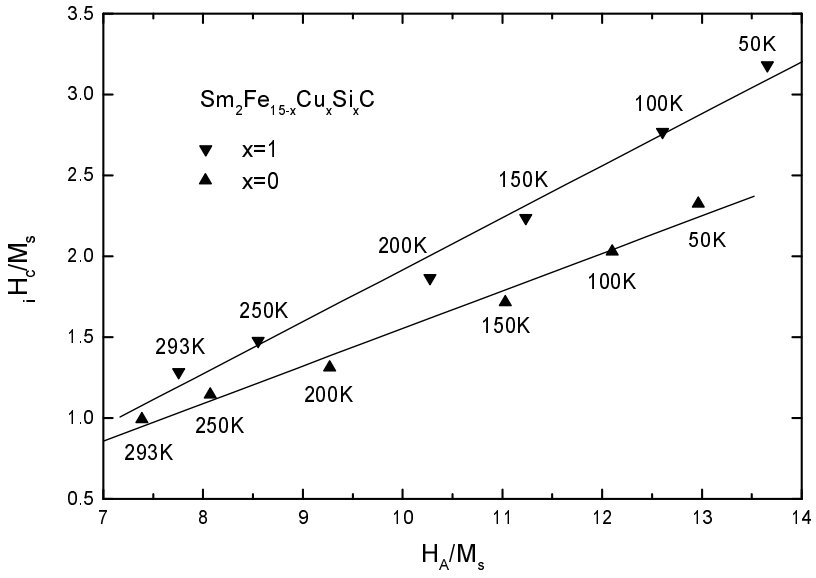

Figure 7. The relation of ${}_i H_c/M_s$ versus H_A/M_s for $Sm_2Fe_{15-x}Cu_xSi_2C$ ($x = 0$ and 1) ribbons obtained at 923 K.

is that atom Cu mainly dopes at the edge of crystalline grains and enhances the resistance of domain wall motivation. A similar phenomenon has been found in melt-spun Pr–Fe–B with Cu addition [24].

Acknowledgment

This work was supported by the National Natural Science Foundation of China.

References

[1] Coey J M D and Sun H 1990 *J. Magn. Magn. Mater.* **87** L251
[2] Zhong X P, Radwanski R J, de Boer F R, Jacobs T H and Buschow K H J 1990 *J. Magn. Magn. Mater.* **86** 333
[3] Shen B G, Kong L S, Wang F W and Cao L 1993 *Appl. Phys. Lett.* **63** 2288
[4] Shen B G, Wang F W, Kong L S, Cao L and Zhan W S 1994 *J. Appl. Phys.* **75** 6253
[5] Cheng Z H, Shen B G, Wang F W, Zhang J X, Gong H Y and Zhao J G 1994 *J. Phys.: Condens. Matter* **6** L185
[6] Hadjipanayis G C, Zheng Y H, Murthy A S, Gong W and Yang F M 1995 *J. Alloys Compounds* **222** 49
[7] Chen Z and Hadjipanayis G C 1997 *J. Magn. Magn. Mater.* **171** 261
[8] van Lier J, Seeger M and Kronmüller H 1997 *J. Magn. Magn. Mater.* **167** 43
[9] Cao L, Handstein A, Grunberger W, Edelman J, Schultz L and Muller K-H 1996 *Appl. Phys. Lett.* **68** 129
[10] Kong L S, Shen B G, Wang F W, Cao L, Guo H Q and Ning T S 1994 *J. Appl. Phys.* **75** 6250
[11] Zhang J X, Cheng Z H and Shen B G 1996 *J. Appl. Phys.* **79** 5528
[12] Zhang H W, Zhang S Y, Shen B G and Zhang L G 1997 *J. Phys. D: Appl. Phys.* **30** 3085
[13] Zhang H W, Zhang S Y, Shen B G and Zhang L G 1998 *J. Appl. Phys.* **83** 4838
[14] Li H S and Hu B P 1998 *J. Physique Coll.* **49** C8 513
[15] Durst K D and Kronmüller H 1986 *J. Magn. Magn. Mater.* **59** 86
[16] Ram U S and Gaunt P 1983 *J. Appl. Phys.* **54** 2872

[17] Kim D H, Kim T K, Park W S and Kim Y B 1996 *J. Magn. Magn. Mater.* **163** 373
[18] Wolf M, Wirth S, Wendhausen P A P, Eckert D and Muller K-H 1995 *J. Magn. Magn. Mater.* **140–144** 995
[19] Buschow K H J 1991 *Rep. Prog. Phys.* **54** 1123–213
[20] Stoner E C and Wohlfarth E P 1948 *Phil. Trans. R. Soc.* **240** 599
[21] Clemente G B, Keem J E and Bradley J P 1988 *J. Appl. Phys.* **64** 5299
[22] Schrefl T, Fidler J and Kronmüller H 1994 *Phys. Rev.* B **49** 6100
[23] Kronmüller K and Schrefl T 1994 *J. Magn. Magn. Mater.* **129** 66
[24] Zhang Y J, Withanawasam L and Hadjipanayis G C 1992 *IEEE Trans. Magn.* **28** 2133